SUPPORTING INFORMATION

Variation of Protein Corona Composition of Gold Nanoparticles Following Plasmonic Heating

Morteza Mahmoudi, [†,‡] Samuel E. Lohse,[†] Catherine J. Murphy,[†] Arman Fathizadeh,[§] Abbas Montazeri,[‖] and Kenneth S. Suslick*[†]*

[†]Department of Chemistry, University of Illinois at Urbana-Champaign, 600 S. Mathews Av., Urbana, Illinois 61801, United States

[‡]Department of Nanotechnology and Nanotechnology Research Center, Faculty of Pharmacy, Tehran University of Medical Sciences, Tehran, Iran

[§]School of Physics, Institute for Research in Fundamental Sciences (IPM), Tehran, Iran

[‖]Faculty of Mechanical Engineering, K.N. Toosi University of Technology, Tehran, Iran

CORRESPONDING AUTHORS:
* Prof. Morteza Mahmoudi. E-mail: Mahmoudi-M@TUMS.ac.ir
* Prof. Kenneth S. Suslick. E-mail: ksuslick@illinois.edu

Materials and Methods

Gold nanorod synthesis. Gold nanorods were synthesized using standard aqueous seeded growth methods.[1] Briefly, small CTAB-stabilized gold nanoparticle seeds were prepared by direct reduction with sodium borohydride, and added to a growth solution containing additional $HAuCl_4$, $AgNO_3$, CTAB, and ascorbic acid.[1] The addition of the gold seed initiates the growth of the gold nanorods, causing the solution to slowly turn a pale brown color, indicating the formation of AuNRs with AR~4. The gold nanorods were purified by centrifugation and washing (11,000 rpm, 14 min. two times) to remove excess gold seed, gold salt, and CTAB. During the second centrifugation cycle, gold nanorods were concentrated to a final concentration of 3.2 nM (with respect to gold nanorods, as determined by UV-vis).[2] The synthesized AuNRs had a longitudinal plasmon absorbance centered at 756 nm.

Preparation of hard corona coated gold nanorods. In order to simulate *in vitro* and *in vivo* media, various concentrations of a diverse protein source were used. Specifically, we incubated gold nanorods in Fetal Bovine Serum (FBS) at FBS concentrations of 10% and 100% FBS, respectively. Gold nanorods were incubated at both plasma concentrations in order to prepare AuNR-FBS complexes. In a typical experiment, 100 μL of gold nanorods (at 3.2 nM) was incubated with 400 μL of proteins at both FBS concentrations for a period of 20 min. at 4 °C; the 10% FBS protein solutions were diluted with PBS buffer. Following the initial incubation, the AuNR-protein solutions were treated with laser-activated hyperthermia or thermal incubation (37 °C, 45 °C). Following treatment, to obtain the hard protein corona complexes (i.e. recovery of the gold nanorods and the tightly bound proteins from the unbound and loosely bound proteins), the incubated samples were centrifuged to pellet the gold nanorods-protein complexes and separated from the supernatant proteins. The pellet was then resuspended in 500 μL of cold PBS (10°C) and centrifuged again for 30 minutes at 20,000 g at 10°C to pellet the nanorod-protein complexes. The standard procedure consists of three washings before re-suspension of the final pellet to the desired concentration. This treatment allows us to remove proteins with low affinity for the nanorod surface (i.e., the soft protein corona).

Hyperthermia experiments. Following the twenty minute incubation at 4°C to allow for formation of the protein corona, AuNR-protein complexes were exposed to continuous laser irradiation for various times. Two types of laser-induced hyperthermia experiments were performed (continuous irradiation for 27.5 min. and 55 min.). Both irradiation experiments used a 785 nm excitation wavelength laser power of ~48 mW and the spot size of ~1.5 mm^2. Following laser irradiation, the hard corona coated AuNRswere isolated according to the centrifugation procedure described in the previous section. The temperature during the hyperthermia experiments was measured by placing a thermocouple in the well and measuring a steady-state temperature at 27.5 min and 55 min of treatment for every sample. Under ambient conditions, the temperature in the well was 26.5 ± 2.2 °C. In the control heating experiments, the "37 °C" water bath had a recorded temperature of 36.8 ± 0.7 °C and the "45 °C" water bath had a recorded temperature of 43.4 ± 0.6 °C. During the hyperthermia experiments, the 10% FBS samples had a mean temperature of 35.0 ± 1.2 °C after 27.5 min. of heating and 39.3 ± 2.9 °C after 55 min., respectively. During the hyperthermia experiments, the 100% FBS samples had a mean temperature of 36.2 ± 1.9 °C after 27.5 min. of heating and 39.6 ± 0.7 °C after 55 min., respectively.

Instrumental analysis. Gold nanorod samples were prepared for TEM analysis by drop-casting AuNR solutions onto SiO/formvar TEM grids (Cu mesh), and the samples were analyzed using a JEOL Cryo 2100 Transmission Electron Microscope. To better visualize the protein corona around the AuNRs, the dropcast AuNR samples were stained with a lanthanum nitrate/osmium tetroxide stain. The surface charge of the AuNP-protein conjugates was analyzed in nanopure deionized water using a Brookhaven Zeta PALS ζ-Potential analyzer. ζ-Potential analysis of the samples was performed on three replicate FBS-AuNR complexes re-suspended in nanopure deionized water. The FBS-AuNR samples for ζ-analysis were prepared and handled by the exact same procedures as the LC-MS samples. UV-vis absorption spectroscopy analysis was performed on a Varian-Cary 500 Scan UV-vis-NIR spectrophotometer.

Liquid chromatography mass spectrometry (LC MS/MS). Nano-particles were spun down by centrifugation at 20,000 x g for 10 minutes and pellet was resuspended in 25 microliters of Sequencing Grade Trypsin (12.5 ng/microliter in 25 mM ammonium bicarbonate, G-Biosciences St. Louis, MO) and digested using a CEM Discover Microwave Digestor (Mathews, NC) for 15 minutes at 55 C (70W). The digestion was stopped by addition of 200 microliters of 50% acetonitrile + 5% formic acid, dried using a Thermo SpeedVac and resuspended in 13 microliters of 5% acetonitrile containing 0.1% formic acid. 10 microliters of sample was used for mass spectroscopy analysis. Mass spectrometer used was a Waters quadrupole time-of-flight mass spectrometer (Q-ToF) connected to a Waters nanoAcquity UPLC. The column used was Waters Atlantis C-18 (0.03 mm particle, 0.075 mm x 150 mm). Flow rate was at 250 nL/min. Peptides were eluted using a linear gradient of water/acetonitrile containing 0.1% formic acid 0-60% B in 240 minutes. The mass spectrometer was set for data dependent acquisition, and MS/MS was performed on the four most-abundant peaks at any given time. Data analysis was done using Waters Protein Lynx Global Server 2.2.5, Mascot (Matrix Sciences) and blasted against NCBI NR database specific for Bostaurus.

In order to obtain the total number of the LC MS/MS spectra for all of the peptides that are attributed to a matched protein, a semi-quantitative assessment of the protein amounts was conducted through application of spectral counting method. The normalized SpC amounts of each protein, identified in the MS study of smooth and jagged surfaces, were calculated by applying the following equation:[3]

$$NpSpC_k = \left(\frac{\left(SpC / (M_w)_k \right)}{\sum_{i=1}^{n} \left(SpC / (M_w)_i \right)} \right) \times 100 \qquad \text{(Eqn. S1)}$$

Where $NpSpC_k$ is the normalized percentage of spectral count (i.e., raw counts of ions) for protein k, SpC is the spectral count identified, and Mw is the molecular weight (in kDa) of the protein k. Using equation S1, one can expect to obtain the protein size and to evaluate the real contribution of each protein to the hard corona composition.[4]

Molecular dynamics. Molecular dynamics (MD) simulations were done with the GROMACS package.[5] The corresponding lipid free structure of the apolipoprotein C-III and apolipoprotein A-I were taken from rcsb.org (pdb accession codes of "2jQ3" and "2A01" respectively). The interactions were defined using CHARMM27 forcefield.[6] 32793and 56314 water molecules were added to the Apo. C-III and Apo. A-I respectively and TIP4P model were used to consider the effect of solvent. Na^+ ions were added to both systems to make them electrically neutralized. First, the systems were minimized by steepest decent algorithm and then both systems were simulated in NPT at temperature of 310 K and pressure of 1atm using Parrinello-Rahman barostat[7] for 200 ps. The time-step was chosen to be 2 fs for all MD simulations. Then the system is simulated at canonical ensemble with stochastic dynamics procedure at 5 different temperatures for 3 ns where the RMSD and R_g were calculated by averaging over the last nanosecond. The simulations were repeated for each temperature by inducing different initial velocities for starting NVT simulations. The error bars in the Figure 5 were calculated from differences in the two simulations at each temperature.

Gradient temperature evaluations. We have considered a natural convection heat transfer problem around a nanorod of radius (R_0) 7 nm and length 40 nm. The surface temperature of the nanorod (T_h) is assumed to be of 45°C (after laser activation) and this heating source is suspended in PBS (Phosphate Buffered Saline) with the temperature equals to 37°C (T_c). It is obvious that the longer the laser pulsed nanorod remains in the fluid, the more volume of the environment would be affected. A relevant question here was to compute the distance R_1 for any heating time (t_h), above which, the fluid temperature could not be any more affected by the nanorod heat source. To this end, the conservation energy equation was employed considering that the fluid temperature was a function of the radial distance (r) and time (t) only.

According to the physical conditions of the problem, the temperature gradient with respect to *r* is linear and thus the temperature profile around the heat source follows a parabola equation. Moreover, this temperature gradient $\left(\frac{dT}{dr}\right)$ should be zero at $r = R_1$ and reach its maximum value at $r = R_0$. Considering these necessary conditions for the temperature variation, this function could be defined as follows:

$$T(r) = \frac{T_h - T_c}{(R_1 - R_0)^2} (R_1 - r)^2 + T_c \qquad \text{(Eqn. S2)}$$

As can be seen, this equation supports the boundary value conditions of the problem, i.e.

$$\begin{cases} at\ r = R_0 & T = T_h = 45°C \\ at\ r = R_1 & T = T_c = 37°C \end{cases} \qquad \text{(Eqn. S3)}$$

Having the temperature variation defined in equation S2, and assuming that the initial temperature of the PBS around the heat source equals to T_c, the total amount of energy needed to increase the temperature of fluid surrounding the nanorod in the zone up to $r = R_1$ could be determined as:

$$Q_{total\ interior} = \int dm.C_p.(T(r) - T_c), \quad dm = 2\pi r dr.\rho \Rightarrow$$
$$Q_{total\ interior} = \int_{R_0}^{R_1} 2\pi r dr.\rho.C_p \left[\frac{T_h - T_c}{(R_1 - R_0)^2} (R_1 - r)^2 \right] \qquad \text{(Eqn. S4)}$$

where the PBS variables are defined as follows. ρ and C_p is the density ($\approx 1\ {}^{g}/_{mol}$) and specific heat capacity of the fluid (4 $\frac{J}{g^{\circ}C}$), respectively. Also, *k* denotes its thermal conductivity equals to 0.6 $\frac{W}{m\,K}$.

On the other hand, the heat flux through the boundary at $r = R_c$ has been determined to be:

$$\dot{Q}|_{exterior} = -kA\frac{\partial T}{\partial r}\Big|_{r=R_c} \qquad \text{(Eqn. S5)}$$

Substituting Equation S2 in S5 yields:

$$\dot{Q}|_{exterior} = 4k\pi R_0(T_h - T_c)\frac{1}{R_c - R_0} \qquad \text{(Eqn. S6)}$$

It is noted that according to the energy conservation rule we have:

$$Q_{total}|_{interior} = \dot{Q}|_{exterior} \cdot t_h \qquad \text{(Eqn. S7)}$$

Solving this equation leads to the time (t_h) needed to affect the fluid temperature at the distance of R_1 by laser pulsed nanorod heating source.

References

1. Furumoto, K.; Ogawara, K.-I.; Nagayama, S.; Takakura, Y.; Hashida, M.; Higaki, K.; Kimura, T. *J. Controlled Rel. of controlled release* **2002,** 83, 89-96.
2. Mahmoudi, M.; Shokrgozar, M. A.; Behzadi, S. *Nanoscale* **2013,** 5, 3240-3244.
3. Monopoli, M. P.; Walczyk, D.; Campbell, A.; Elia, G.; Lynch, I.; Baldelli Bombelli, F.; Dawson, K. A. *J. Am. Chem. Soc.***2011,** 133, 2525-2534.
4. Walczyk, D.; Bombelli, F. B.; Monopoli, M. P.; Lynch, I.; Dawson, K. A. *J. Am. Chem. Soc.***2010,** 132, 5761-5768.
5. Hess, B.; Kutzner, C.; Van Der Spoel, D.; Lindahl, E. *J. Chem. Theory Comput.* **2008**, 4, 435–447.
6. Bjelkmar P, Larsson P, Cuendet MA, Hess B, Lindahl E *J. Chem. Theory Comput.* **2010**, 6, 459–466.
7. Parrinello, M.; Rahman, A. *J. Appl. Phys.* **1981**, 52, 7182.

Composition of Protein Corona from LC MS/MS

Table S1. Representative hard corona proteins associated with AuNRs incubated in 10% FBS for different thermal and photothermal treatments (incubation at 37°C, 45°C, and continuous laser irradiation), as identified by LC MS/MS[a]; standard deviations were obtained from three individual tests.

Molecular Weight (kDa)	Protein name	NSpC			
		37°C	Heated at 45°C	Continuous laser (27.5 min)	Continuous laser (55 min)
69	serum albumin	5.4±0.1	3.8±1.1	9.8±2	9.4±0.7
46	α-1-antiproteinase precursor	4.2±0.2	6.1±3	6.4±0.7	7.1±0.6
38	α-2-HS-glycoprotein precursor	7.7±1.6	3.8±1.9	10.0±0.7	14.2±1.8
30	apolipoprotein A-I precursor	15±5	10.0±3.	6.9±3	8.4±0.3
16	hemoglobin fetal subunit beta	10±4	13.9±0.4	9.5±1.9	13±2
15	Hemoglobin	5.5±1.6	18±5	4.8±3	5.6±1.6
11	apolipoprotein A-II precursor	5.9±0.2	7.5±1.1	7.1±0.7	12.5±2.5
11	apolipoprotein C-III precursor	2.5±0.2	2.9±0.1	4.1±0.1	6.0±1.0

[a]Normalized spectral count (NSpC) values were calculated for each protein hit according to the equation S1 in the SI Materials and Methods section. This table contains only the most significant hits, while the full list of the most abundant proteins identified by LC MS/MS is given in SI Table S3.

Table S2. Representative hard corona proteins associated with AuNRs incubated in 100% FBS for different thermal and photothermal treatments (incubation at 37°C, 45°C, and continuous laser irradiation), as identified by LC MS/MS[a]; standard deviations were obtained from three individual tests.

Molecular Weight(kDa)	Protein name	NSpC			
		37°C	Heated at 45°C	Continuous laser (27.5 min)	Continuous laser (55 min)
69	serum albumin	8.7±3.1	6.7±1.5	9.1±3.1	6.6±1.6
46	α-1-antiproteinase precursor	5.6±1.5	4.8±0.9	4.1±0.3	4.8±0.6
38	α-2-HS-glycoprotein precursor	14.6±1.2	6.1±0.1	11±3	11.2±1.4
30	apolipoprotein A-I precursor	4.2±0.9	8.4±2.0	3.6±1.0	4.2±0.1
16	hemoglobin fetal subunit beta	17±7	9.8±1.8	12±3	9±2
15	Hemoglobin	7.6±0.7	14±5	4.8±0.7	3.7±0.7
11	apolipoprotein A-II precursor	21.0±1.5	3.9±0.6	5.5±0.1	6±1
11	apolipoprotein C-III precursor	0.5±0.6	3.1±0.8	2.3±1.2	1.9±0.8

[a]Normalized spectral count (NSpC) values were calculated for each protein hit according to the equation S1 of Materials and Methods section of SI. This table contains only the most significant hits, while the full list of the most abundant proteins identified by LC MS/MS is given in SI Table S4.

Table S3: List of all prominent proteins identified in the hard corona associated with AuNRs incubated in 10% FBS at different situations (incubation at 37°C, 45°C, and after continuous laser irradiation for 27 and 55 min.)

Molecular Weight (Da)	Protein name	NSpC			
		37°C	Heat (45°C)	Laser 27 min	Laser 55 min
271983	Fibronectin	0.28±0.03	0.07±0.01	0.14±0.01	0.10±0.03
228958	myosin-10	0.14±0.09	0.03±0.01	0.11±0.06	0.11±0.01
192676	complement C4 precursor	1.02±0.15	0.02±0.01	0.13±0.09	0.10±0.02
187112	complement C3 preproprotein	1.33±0.21	0.05±0.01	0.38±0.04	0.12±0.01
167470	alpha-2-macroglobulin	1.63±0.36	0.73±0.16	1.35±0.52	1.18±0.96
129451	thrombospondin-1 precursor	0.11±0.06	0.02±0.01	0.10±0.01	0.13±0.02
106120	inter-alpha-trypsin inhibitor heavy chain H2 precursor	1.28±0.71	1.20±0.15	1.66±0.62	0.75±0.28
101449	inter-alpha-trypsin inhibitor heavy chain H4 precursor	1.27±0.11	0.45±0.02	1.31±0.71	0.78±0.25
99187	inter-alpha (globulin) inhibitor H3	0.88±0.08	0.11±0.01	0.25±0.11	0.31±0.28
93075	periostin	0.37±0.14	0.02±0.01	0.12±0.08	0.12±0.04
88254	cadherin-6 precursor	0.72±0.19	0.11±0.01	0.12±0.02	0.10±0.01
85634	gelsolin isoform a precursor	1.33±0.23	0.09±0.01	1.43±0.79	0.25±0.13
77703	Serotransferrin	0.29±0.14	0.04±0.01	0.90±0.13	0.10±0.01
70461	Prothrombin	0.71±0.17	0.07±0.01	0.74±0.13	0.11±0.04
69248	Serum albumin	5.43±0.10	3.76±1.11	9.75±2.05	9.42±0.70
68847	Kininogen-1	0.35±0.01	0.12±0.01	0.43±0.32	0.12±0.01
68543	alpha-fetoprotein precursor	0.23±0.01	0.09±0.01	0.20±0.12	0.16±0.02
55172	heparin cofactor 2 precursor	0.27±0.12	0.05±0.01	0.34±0.29	0.10±0.01
54676	alpha-2-antiplasmin precursor	0.81±0.02	0.15±0.01	0.79±0.41	0.36±0.14
53520	alpha-1B-glycoprotein precursor	0.73±0.13	0.05±0.01	0.33±0.13	1.10±0.57
53307	vitamin D-binding protein precursor	0.98±0.00	0.16±0.04	1.42±0.12	1.61±0.75
53278	angiopoietin-related protein 3 precursor	0.27±0.32	0.09±0.01	0.34±0.17	0.11±0.01
51081	clusterinpreproprotein	1.36±0.40	1.04±0.10	0.41±0.29	0.41±0.32
48931	cartilage oligomeric matrix protein	0.10±0.07	0.09±0.01	0.11±0.05	0.10±0.04
48469	fibrinogen beta chain	0.20±0.12	0.17±0.04	0.16±0.12	0.12±0.03
47607	adenosylhomocysteinase	0.13±0.03	0.06±0.01	0.16±0.11	0.11±0.03
46075	alpha-1-antiproteinase precursor	4.22±0.24	6.05±3.33	6.37±0.7	7.08±0.59
45428	angiotensinogen precursor	1.45±0.12	1.17±0.28	0.26±0.12	0.11±0.02
42991	apolipoprotein A-IV precursor	1.18±0.08	0.16±0.02	0.11±0.04	0.53±0.31
42906	fibromodulin precursor	0.16±0.06	0.06±0.01	0.11±0.02	0.12±0.02
42636	fetuin-B precursor	1.34±0.16	0.35±0.30	1.19±0.01	1.68±0.40
42024	actin	0.55±0.11	0.41±0.39	0.21±0.13	0.10±0.01
41905	fibrinogen A-alpha chain	1.55±0.91	0.85±0.25	0.10±0.03	1.31±0.02
38732	lumican precursor	0.53±0.14	1.23±0.38	0.18±0.03	0.11±0.02
38394	alpha-2-HS-glycoprotein precursor	7.71±1.57	3.77±1.86	10.02±0.73	14.17±1.79
33286	regucalcin	0.50±0.18	0.09±0.01	0.11±0.07	0.13±0.01
31388	N-acetylglucosamine-1-phosphotransferase subunit gamma	0.64±0	0.11±0.01	0.16±0.13	0.10±0.03
30258	apolipoprotein A-I preproprotein	14.95±4.90	9.97±3.29	6.88±2.97	8.40±0.28
24444	anti-testosterone antibody	0.74±0.15	0.09±0.01	0.11±0.01	0.11±0.01
23168	alpha-1-acid glycoprotein precursor	0.48±0.20	0.21±0.11	0.35±0.22	1.44±0.01
22731	secreted phosphoprotein 24 precursor	0.95±0.16	0.11±0.01	0.58±0.23	0.12±0.02
22697	alpha1-antichymotrypsin isoform pHHK11, partial	0.52±0.15	0.06±0.01	0.11±0.02	0.11±0.01
22665	heat shock protein beta-1	0.56±0.10	0.45±0.44	0.26±0.12	0.13±0.02
15849	hemoglobin fetal subunit beta	9.72±3.85	13.88±0.39	9.51±1.89	13.12±2.06
15044	Hemoglobin	5.50±1.59	18.4±5.09	4.84±2.51	5.60±1.63
14678	serum amyloid A-4 protein precursor	0.45±0.26	0.11±0.01	0.43±0.12	0.11±0.01
11195	apolipoprotein A-II precursor	5.89±0.17	7.49±1.08	7.12±0.68	12.51±2.51
11054	apolipoprotein C-II precursor	0.34±0.11	2.06±1.20	0.32±0.21	0.44±0.17
10685	apolipoprotein C-III precursor	2.45±0.22	2.90±0.01	4.14±0.02	6.02±1.02
1439	hypoxia-associated protein	3.48±2.46	0.12±0.21	2.25±0.09	0.11±0.02

Table S4: List of all prominent proteins identified in the hard corona associated with AuNRs incubated in 100% FBS at different situations (incubation at 37°C, 45°C, and after continuous laser irradiation for 27 and 55 min.).

Molecular Weight (Da)	Protein name	NSpC			
		37°C	Heat (45°C)	Laser 27 min	Laser 55 min
271983	Fibronectin	0.55±0.68	0.25±0.07	0.21±0.11	0.13±0.04
228958	myosin-10	0.53±0.51	0.34±0.02	0.03±0.01	0.07±0.02
192676	complement C4 precursor	0.31±0.01	0.09±0.01	0.05±0.01	0.22±0.10
187112	complement C3 preproprotein	0.18±0.17	0.75±0.10	0.42±0.17	0.58±0.06
167470	alpha-2-macroglobulin	0.26±0.25	1.16±0.09	0.66±0.03	0.79±0.25
129451	thrombospondin-1 precursor	0.69±0.06	0.06±0.05	0.10±0.01	0.16±0.03
106120	inter-alpha-trypsin inhibitor heavy chain H2 precursor	0.56±0.38	1.22±0.46	0.77±0.44	0.04±0.03
101449	inter-alpha-trypsin inhibitor heavy chain H4 precursor	2.03±0.01	0.5±0.27	0.98±0.43	1.28±0.10
99187	inter-alpha (globulin) inhibitor H3	0.17±0.05	0.16±0.13	0.22±0.01	0.13±0.01
93075	periostin	0.18±0.06	0.08±0.01	0.06±0.01	0.13±0.01
88254	cadherin-6 precursor	0.32±0.35	0.12±0.01	0.07±0.01	0.73±0.08
85634	gelsolin isoform a precursor	0.81±0.23	0.10±0.01	0.01±0.01	0.88±0.12
77703	Serotransferrin	1.15±0.07	0.13±0.01	0.15±0.01	0.07±0.02
70461	Prothrombin	1.19±0.17	0.94±0.21	0.09±0.01	0.51±0.09
69248	Serum albumin	7.72±3.10	6.69±1.50	9.12±3.05	6.57±1.58
68847	Kininogen-1	0.37±0.08	0.45±0.31	0.10±0.05	0.37±0.07
68543	alpha-fetoprotein precursor	0.15±0.07	0.11±0.01	0.04±0.01	0.11±0.01
55172	heparin cofactor 2 precursor	0.21±0.14	0.13±0.04	0.03±0.01	0.61±0.07
54676	alpha-2-antiplasmin precursor	0.22±0.14	0.13±0.04	0.28±0.05	0.16±0.02
53520	alpha-1B-glycoprotein precursor	1.2±0.24	0.36±0.13	0.98±0.17	1.10±0.15
53307	vitamin D-binding protein precursor	0.47±0.09	0.12±0.01	0.39±0.09	0.48±0.07
53278	angiopoietin-related protein 3 precursor	0.32±0.15	0.09±0.01	0.03±0.01	0.11±0.01
51081	clusterinpreproprotein	0.43±0.14	0.71±0.03	0.27±0.01	0.58±0.03
48931	cartilage oligomeric matrix protein	0.27±0.05	0.08±0.01	0.06±0.01	0.05±0.01
48469	fibrinogen beta chain	0.58±0.08	0.39±0.08	0.03±0.01	0.12±0.03
47607	adenosylhomocysteinase	0.95±0.24	0.09±0.01	0.10±0.03	0.10±0.02
46075	alpha-1-antiproteinase precursor	5.6±1.49	4.76±0.93	4.07±0.33	4.82±0.64
45428	angiotensinogen precursor	0.18±0.08	0.96±0.08	0.37±0.12	0.29±0.09
42991	apolipoprotein A-IV precursor	0.7±0.07	0.09±0.01	0.07±0.01	0.39±0.05
42906	fibromodulin precursor	0.31±0.02	0.12±0.01	0.14±0.01	1.06±0.56
42636	fetuin-B precursor	0.49±0.06	1.08±0.94	1.16±0.32	1.06±0.56
42024	actin	0.32±0.15	0.12±0.01	0.01±0.01	0.16±0.06
41905	fibrinogen A-alpha chain	0.38±0.07	0.09±0.01	0.52±0.23	0.16±0.06
38732	lumican precursor	0.32±0.01	0.17±0.07	0.14±0.09	0.15±0.05
38394	alpha-2-HS-glycoprotein precursor	14.58±1.22	6.13±0.05	11.06±3.01	11.16±1.39
33286	regucalcin	0.63±0.15	0.09±0.01	0.01±0.01	0.11±0.01
31388	N-acetylglucosamine-1-phosphotransferase subunit gamma	0.85±0.38	0.06±0.01	0.09±0.01	0.11±0.02
30258	apolipoprotein A-I preproprotein	4.15±0.91	8.37±1.96	3.58±0.98	4.21±0.02
24444	anti-testosterone antibody	0.70±0.07	0.47±0.39	0.04±0.01	0.14±0.03
23168	alpha-1-acid glycoprotein precursor	0.49±0.06	0.64±0.20	0.44±0.19	0.48±0.10
22731	secreted phosphoprotein 24 precursor	0.36±0.09	0.67±0.40	0.11±0.01	0.50±0.05
22697	alpha1-antichymotrypsin isoform pHHK11, partial	0.16±0.06	0.02±0.01	0.01±0.01	0.45±0.11
22665	heat shock protein beta-1	0.08±0.01	0.01±0.01	0.06±0.01	0.13±0.04
15849	hemoglobin fetal subunit beta	16.65±7.04	9.81±1.79	12.31±2.96	9.66±2.44
15044	Hemoglobin	7.55±0.70	14.14±4.91	4.78±0.72	3.71±0.70
14678	serum amyloid A-4 protein precursor	0.07±0.03	0.51±0.02	0.07±0.01	0.15±0.04
11195	apolipoprotein A-II precursor	20.95±1.46	3.92±0.57	5.52±0.05	6.01±1.01
11054	apolipoprotein C-II precursor	0.51±0.58	3.19±0.50	1.04±0.35	0.82±0.09
10685	apolipoprotein C-III precursor	0.52±0.57	3.12±0.75	2.27±1.18	1.88±0.79
1439	hypoxia-associated protein	1.97±0.11	2.74±1.2	1.93±0.69	0.45±0.62

Table S5. Normalized spectral counts (NSpC) of proteins of various molecular weights ranges contained in the hard corona incubated for 1 h in 10% and 100% FBS solutions under different conditions (*i.e.* incubation at 37°C, 45°C,continuous-lasers).

Molecular Weight (kDa)	10% FBS solution				100% FBS solution			
	37°C	45°C	Continuous (27.5 min)	Continuous (55 min)	37°C	45°C	Continuous (27.5 min)	Continuous (55 min)
<30	31±7	37±2	38±1	48±8	50±9	30±7	24±1	45±1
30-50	42±4	32±2	35±1	27±11	30±3	22±9	24±3	29.7±0.8
50-70	10.5±1.2	19.0±1.8	14.6±3.2	7±2	11±3	11±5	10.1±1.4	14.8±1.0
70-100	4.4±0.6	4.3±0.6	10.9±0.4	0.45±0.1	3.8±0.9	1.8±0.5	2.5±0.1	2.2±1.0
100-500	7.4±1.2	5.9±1.6	2.9±1.2	2.2±0.1	5.2±1.6	3.7±0.1	3.3±0.5	5.4±0.5

Table S6. LSPR λ_{max} Data for AuNR-protein Complexes Under Different Heating Conditions

Sample Name	LSPR λ_{max} (nm)
CTAB-AuNRs	756.0 ± 2.5
CTAB-AuNRs (post laser irradiation)	755.4 ± 1.7
10% FBS AuNRs (no irradiation)	736.0 ± 2.0
100% FBS AuNRs (no irradiation)	731.2 ± 2.6
10% FBS AuNRs (37 °C)	728.3 ± 0.6
10% FBS AuNRs (45 °C)	729.5 ± 2.1
10% FBS AuNRs (27.5 min.)	732.4 ± 2.9
10% FBS AuNRs (55 min.)	734.1 ± 2.5
100% FBS AuNRs (37 °C)	729.5 ± 2.8
100% FBS AuNRs (45 °C)	730.0 ± 2.0
100% FBS AuNRs (27.5 min.)	727.0 ± 1.8
100% FBS AuNRs (55 min.)	728.2 ± 2.8

Table S7. Heating time (t_h) needed to affect the fluid temperature at the distance of R_1 by laser pulsed nanorod heating source.

R_1 (m)	t_h (s)
5.7E-08	**3.39E-09**
1.07E-07	**9.74E-09**
5.07E-07	**5.39E-07**
1.01E-06	**2.74E-06**
2.01E-06	**1.55E-05**
5.01E-06	**0.000181**
1E-05	**0.001135**
2E-05	**0.007353**
3E-05	**0.020696**
4E-05	**0.041877**
5E-05	**0.071122**
6E-05	**0.108467**
7E-05	**0.153875**
8E-05	**0.207276**
9E-05	**0.268593**
0.0001	**0.337746**
0.0002	**2.480389**
0.0003	**7.71482**
0.0004	**16.92494**
0.0005	**30.72278**
0.0006	**49.53599**
0.0007	**73.66575**
0.0008	**103.3252**
0.0009	**138.6655**
0.001	**179.7936**

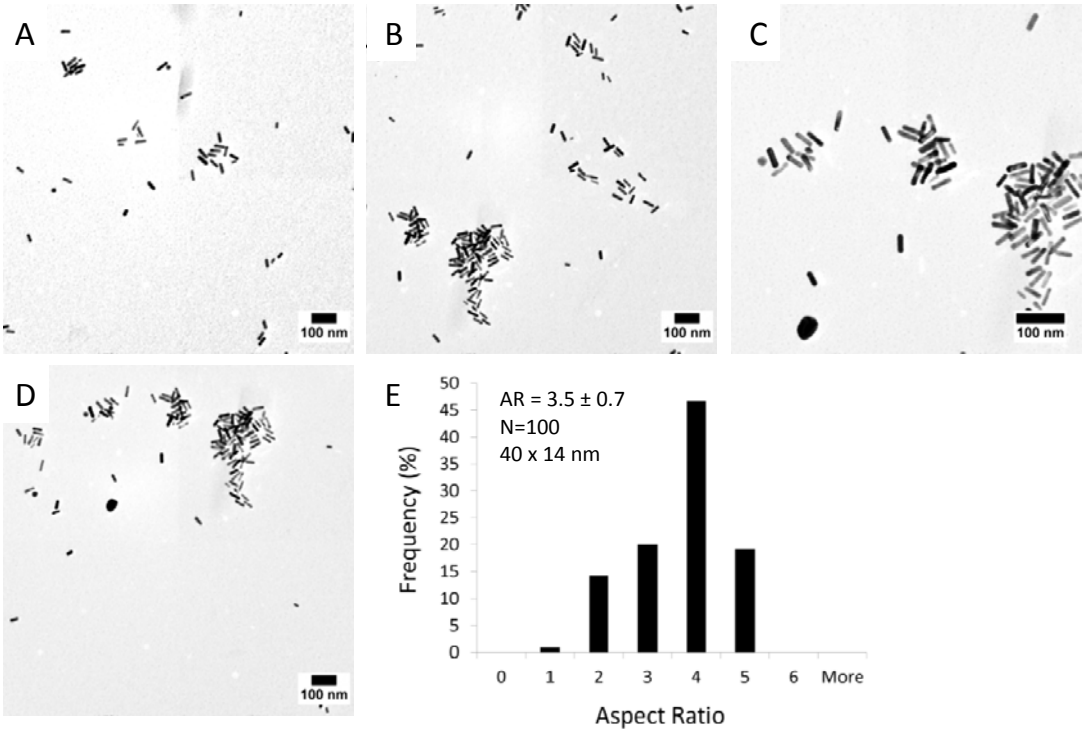

Figure S1. TEM Images and aspect ratio analysis of the gold nanorods used in this study. (A-D) Representative TEM Images of the AuNRs. Scale bars are 100 nm. (E) Aspect ratio analysis of the CTAB-AuNRs. The mean aspect ratio of AuNRs is 3.5 ± 0.7 (N = 100) and the mean dimensions are 40 x 14 nm.

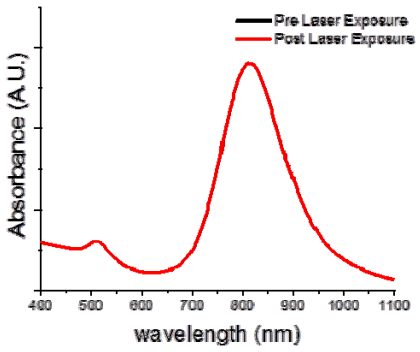

Figure S2. UV-vis absorbance spectra of CTAB-AuNRs before and after 55 min. of continuous laser irradiation. The laser irradiation induces no change in the absorbance spectrum of the AuNR solution, and therefore no change in the AuNR shape.

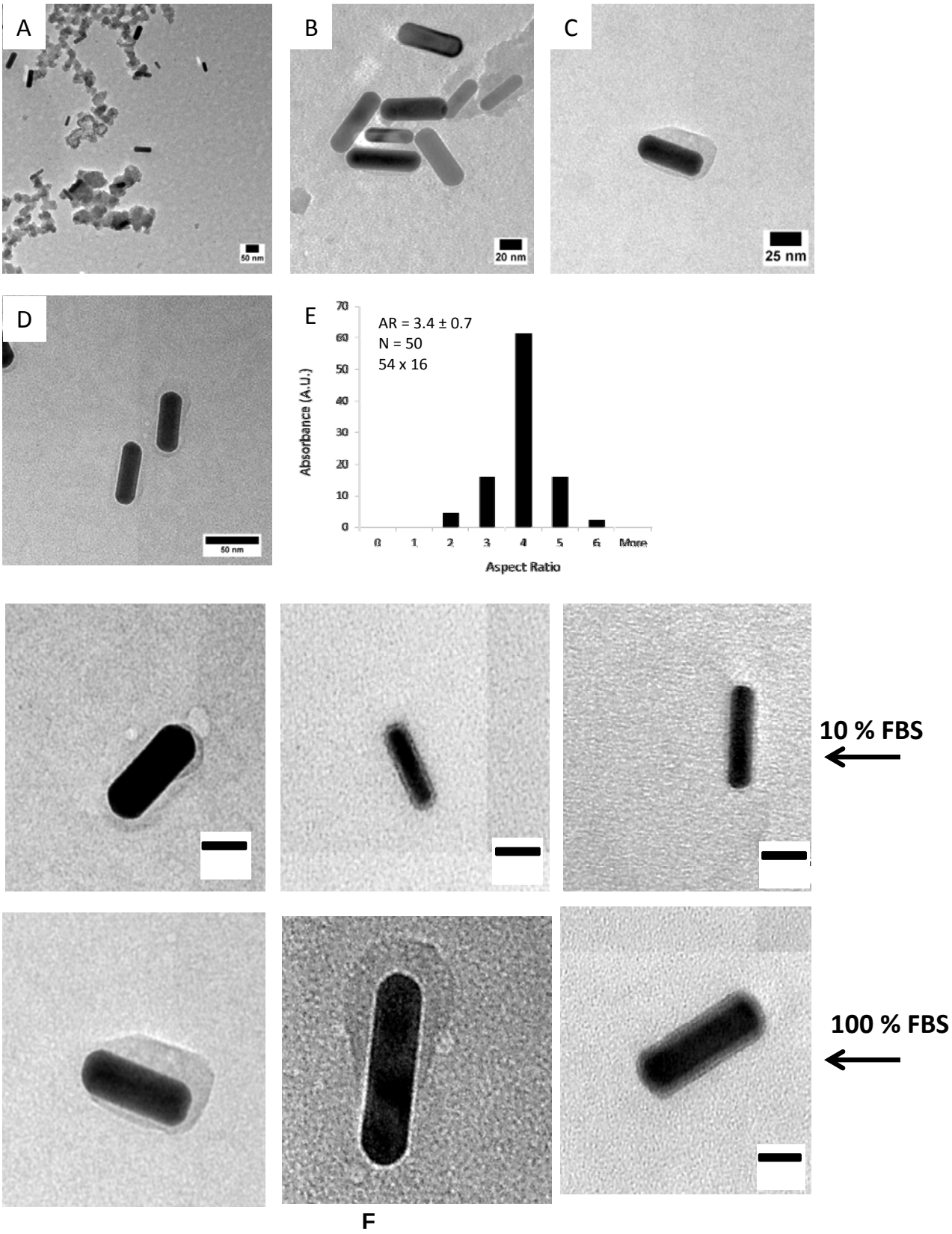

Figure S3. TEM images of individual protein-AuNR hard corona conjugates visualized using an osmium tetroxide/lanthanum nitrate stain. (A-C) 10% FBS-AuNR conjugates. Scale bars are 50, 20, 25 nm, respectively. (D) 100% FBS-AuNR conjugates. Scale bar is 50 nm. (E) Aspect ratio analysis of protein-AuNR conjugates; (F) higher resolution TEM image of the individual protein coated AuNR at various protein concentrations (scale bars are 20 nm)

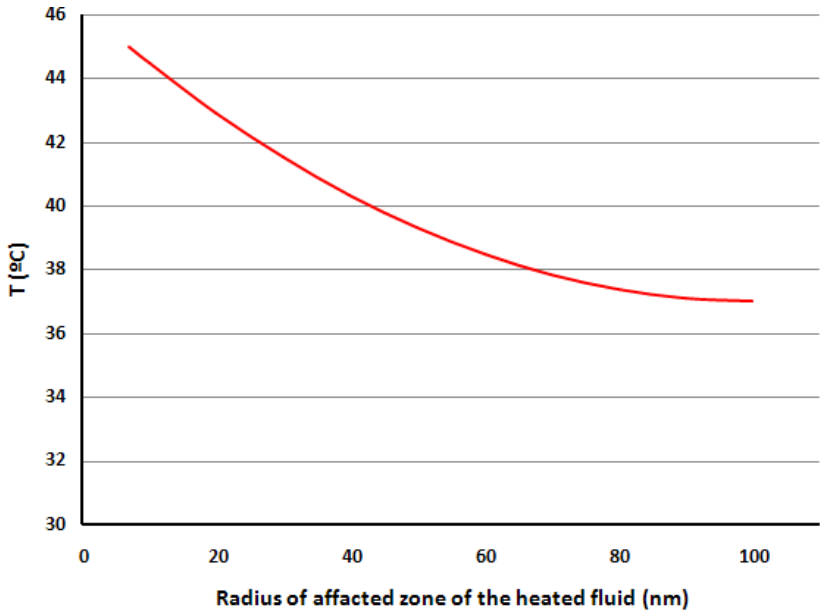

(a)

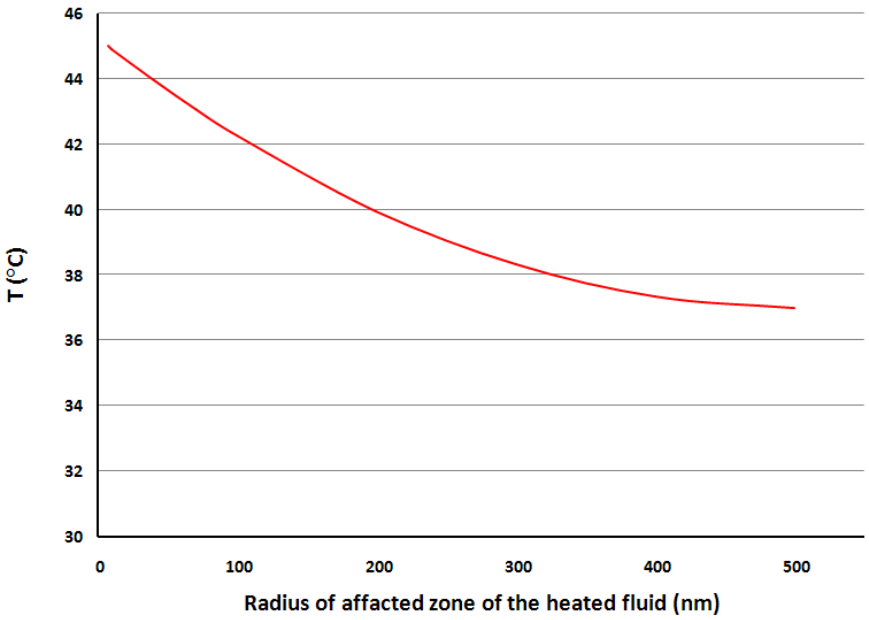

(b)

Figure S4. Temperature changes from the nanorod surface to the maximum radius of the heated fluid of (a) 100 nm in the case of 10 nanoseconds heating and (b) 500 nm for 540 nanoseconds heating.